

Species-specific Differences of the Spectroscopic Properties of P700

ANALYSIS OF THE INFLUENCE OF NON-CONSERVED AMINO ACID RESIDUES BY SITE-DIRECTED MUTAGENESIS OF PHOTOSYSTEM I FROM *CHLAMYDOMONAS REINHARDTII**

Received for publication, May 7, 2003, and in revised form, August 20, 2003
Published, JBC Papers in Press, August 21, 2003, DOI 10.1074/jbc.M304776200

Heike Witt^{‡§}, Enrica Bordignon[¶], Donatella Carbonera[¶], Jan P. Dekker^{||},
Navassard Karapetyan^{**}, Christian Teutloff[‡], Andrew Webber^{‡‡}, Wolfgang Lubitz^{‡§§},
and Eberhard Schlodder^{‡¶¶}

From the [‡]Max-Volmer-Laboratorium für Biophysikalische Chemie, Technische Universität Berlin, Strasse des 17. Juni 135, 10623 Berlin, Germany, [¶]Dipartimento di Chimica Fisica, Università di Padova, Via Loredan 2, 35131 Padova, Italy, ^{**}A. N. Bakh Institute of Biochemistry, Russian Academy of Sciences, Leninsky Prospect, 33, 119071 Moscow, Russia, the ^{||}Department of Physics and Astronomy, Vrije Universiteit, De Boelelaan 1081, 1081 HV Amsterdam, The Netherlands, ^{‡‡}Center for the Study of Early Events in Photosynthesis, the Department of Plant Biology, Arizona State University, Tempe, Arizona 85287-1601, and ^{§§}MPI für Bioorganische Chemie, Stiftstrasse 34-36, 45470 Mülheim/Ruhr, Germany

We applied optical spectroscopy, magnetic resonance techniques, and redox titrations to investigate the properties of the primary electron donor P700 in photosystem I (PS I) core complexes from cyanobacteria (*Thermosynechococcus elongatus*, *Spirulina platensis*, and *Synechocystis* sp. PCC 6803), algae (*Chlamydomonas reinhardtii* CC2696), and higher plants (*Spinacia oleracea*). Remarkable species-specific differences of the optical properties of P700 were revealed monitoring the (³P700–P700) and (P700⁺–P700) absorbance and CD difference spectra. The main bleaching band in the Q_y region differs in peak position and line width for the various species. In cyanobacteria the absorbance of P700 extends more to the red compared with algae and higher plants which is favorable for energy transfer from red core antenna chlorophylls to P700 in cyanobacteria. The amino acids in the environment of P700 are highly conserved with two distinct deviations. In *C. reinhardtii* a Tyr is found at position PsaB659 instead of a Trp present in all other organisms, whereas in *Synechocystis* a Phe is found instead of a Trp at the homologous position PsaA679. We constructed several mutants in *C. reinhardtii* CC2696. Strikingly, no PS I could be detected in the mutant YW B659 indicating steric constraints unique to this organism. In the mutants WA A679 and YA B659 significant changes of the spectral features in the (³P700–P700), the (P700⁺–P700) absorbance difference and in the (P700⁺–P700) CD difference spectra are induced. The results indicate structural differences among PS I from higher plants, algae, and cyanobacteria and give further insight into specific protein-cofactor interactions contributing to the optical spectra.

Photosystem I (PS I)¹ is a multisubunit pigment-protein complex located in the thylakoid membranes of cyanobacteria,

algae, and plants that mediates light-induced electron transfer from plastocyanin or cytochrome *c*₆ on the luminal side to ferredoxin on the stromal side (for a review see Refs. 1 and 2). In plants and algae, PS I is composed of the core complex and the light-harvesting complex LHCI. LHC I complexes do not exist in cyanobacteria. The PS I core complexes of all organisms consist of two large subunits, PsaA and PsaB, and at least eight smaller subunits (3). However, some differences between the cyanobacterial and chloroplast PS I core complexes exist. (i) In cyanobacteria, two additional small subunits, PsaM and PsaX, are found not present in algae and plants, which instead contain another four additional subunits, PsaH, PsaG, PsaN, and PsaO, not found in cyanobacteria (4, 5). (ii) Trimer formation of PS I is common for cyanobacteria but is not observed in algae and plants. (iii) Another difference can be found regarding the type of electron carrier proteins used to transfer electrons to the oxidized primary donor P700⁺ and their interaction with PS I (6). In *Thermosynechococcus elongatus*, cytochrome *c*₆ is the only electron carrier, whereas in *Chlamydomonas reinhardtii* cytochrome *c*₆ or plastocyanin can be used, mainly depending on the nutrient conditions (7).

Although only the three-dimensional structure of PS I from *T. elongatus* is known (8), it is generally assumed that the PS I core complexes, and especially the cofactor arrangement in the reaction center, are similar in all organisms despite the differences described above. The two large subunits, PsaA and PsaB, each consisting of 11 transmembrane helices, form the heterodimeric catalytic core and coordinate most of the cofactors involved in the electron transfer process except for the terminal electron acceptors F_A and F_B (two [4Fe-4S] iron-sulfur clusters) that are bound by one of the extrinsic subunits on the stromal side, PsaC. Besides the reaction center, this heterodimer harbors the core antenna system, together with some of the smaller integral subunits, consisting of about 100 chlorophylls and 20 β -carotenes. The primary sequences of these

* This work was supported by Sfb 498 TPC5 and TPA6 and the TMR Programme FMRX-CT98–0214. The costs of publication of this article were defrayed in part by the payment of page charges. This article must therefore be hereby marked “advertisement” in accordance with 18 U.S.C. Section 1734 solely to indicate this fact.

§ To whom correspondence may be addressed: Max-Volmer-Laboratorium für Biophysikalische Chemie. Tel.: 49-30-31425968; Fax: 49-30-31421122; E-mail: h.witt.berlin@web.de.

¶¶ To whom correspondence may be addressed: Max-Volmer-Laboratorium für Biophysikalische Chemie. Tel.: 49-30-31422688; Fax: 49-30-31421122; E-mail: eber0535@mailbox.tu-berlin.de.

¹ The abbreviations used are: PS I (II), photosystem I (II); ADMR,

absorption-detected magnetic resonance; B_A and B_B, accessory chlorophylls ligated by subunit PsaA and PsaB, respectively; CAPS, 3-(cyclohexylamino)-1-propanesulfonic acid; Chl, chlorophyll; β -DM, *n*-dodecyl β -maltoside; ENDOR, electron nuclear double resonance; hfc, hyperfine coupling constant; LHC, light-harvesting complex; P700, primary electron donor of PS I; P700⁺, cation radical of P700; ³P700, triplet state of P700; P_A and P_B, the two chlorophylls constituting P700 ligated by subunit PsaA and PsaB, respectively; T-S, triplet-minus-singlet; Tricine, *N*-[2-hydroxy-1,1-bis(hydroxymethyl)ethyl]glycine; TMPD, tetramethyl-*p*-phenylenediamine dihydrochloride; ZFS, zero field-splitting.

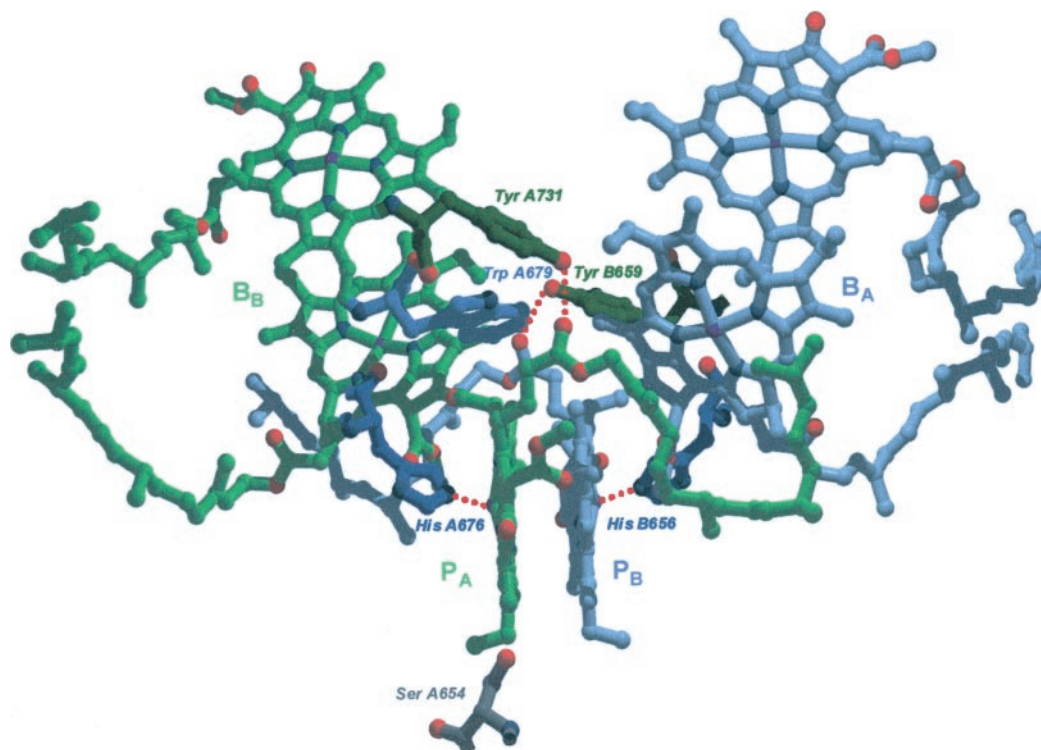


FIG. 1. **Proposal for amino acid residues in the vicinity of the primary donor P700 in *C. reinhardtii*.** The figure was drawn on the basis of the coordinates of the PS I structure of *T. elongatus* (8), with numbering according to *C. reinhardtii*; the two non-conserved amino acid residues have been replaced in the PS I structure of *T. elongatus* (8) by Tyr at position B659 and Ser at position A654 by using the program Swiss PdbViewer. Tyr-A731 and Tyr-B659 are putative hydrogen bond donors to the keto-carbonyl groups of the phytyl side chains of P_A and P_B, respectively. Also depicted in the figure are His-A676 and His-B656 as the coordinating ligands to P700 and Trp at position A679 which is the homologous one to B659 on PsaA. The additional chlorophylls in the two branches are also shown. View direction is perpendicular to the membrane normal.

large subunits are highly conserved and the same holds for the primary photochemistry of the reaction center of PS I, although there is a discussion going on that in some species both branches participate in the primary charge separation whereas in other species only the A-branch seems to be active (9, 10).

After absorption of light by an antenna pigment, the excitation energy is transferred to the primary electron donor P700, a chlorophyll *a* dimer. P700 being in the lowest excited singlet state donates an electron to the primary electron acceptor A₀, a chlorophyll *a* monomer. Charge stabilization is achieved by subsequent electron transfer to secondary acceptors, the phylloquinone A₁ and Fx, a [4Fe-4S] iron-sulfur cluster and finally to F_A and F_B. The x-ray crystallographic analysis of cyanobacterial PS I (8) has revealed that the primary electron donor P700 of photosystem I is a dimer composed of one chlorophyll *a* and one chlorophyll *a*' that is the 13² epimer of Chl *a*. The coordinating ligand of Chl *a*' (P_A) is provided by a His from PsaA (His-A676) (numbering according to *Chlamydomonas* throughout the text), whereas the one of Chl *a* (P_B) is provided by PsaB (His-B656). Based on ENDOR spectra of P700⁺, which exhibit nearly identical hyperfine coupling constants of the methyl protons of all investigated species, it has been concluded that the positive charge is mainly localized on P_B (11–14).

Despite the remarkable similarities described above, optical spectroscopy of PS I complexes from different species indicates considerable differences. For example, although the flash-induced (P700⁺-P700) absorbance difference spectra of *T. elongatus* and *Spinacia oleracea* (spinach) are rather similar (15, 16), those recorded for *Anabaena variabilis* (15) and *C. reinhardtii* (17, 18) look different.

To investigate the reasons for species-specific differences, we were looking for differences in the primary sequences. In all

organisms sequenced so far, the amino acid residues around P700 are highly conserved. Based on the 2.5-Å structure of PS I from *T. elongatus*, we searched for all amino acids located within a distance of 10 Å with respect to the magnesium atoms of P_A and P_B. The sequence comparison shows that the respective amino acids are identical for *T. elongatus* and spinach. Two differences exist between *C. reinhardtii* and *T. elongatus*. A Ser is found at position A654 instead of an Ala in *T. elongatus*. The exchange of this Ala against Ser using the program Swiss PdbViewer indicates that the Ser could be located close to P_A between the vinyl and methyl side chains. Although the polarity of the binding pocket of P_A might be slightly higher for *C. reinhardtii*, we do not expect that this amino acid residue has a significant influence on the optical properties of P700. A striking difference is a Tyr at position B659 in *C. reinhardtii*, whereas a Trp is conserved in all other organisms. For *Synechocystis* three differences are found, namely Gly instead of Ala-A675, Phe instead of Leu-A622, and a Phe is present at position A679 which is the homologous position to B659 on PsaA where Trp is always found in the other organisms. We did not investigate further the differences found for *Synechocystis* due to the mutagenesis system chosen (see below). Unfortunately, the amino acid sequence of *Spirulina platensis* is not available so far. The amino acid residues at positions B659 and A679 are the most interesting ones due to their close vicinity to P700 and the accessory Chls (within 4 Å). An additional interesting aspect of these residues is their location one helix turn toward the stromal side with respect to the coordinating ligands, forming a roof-like structure orthogonal to P700 (Fig. 1). In *C. reinhardtii*, the Tyr-B659 might be able to form a hydrogen bond to the keto group of the phytyl side chain of P_B. This would be analogous to the proposal based on the crystal structure that the conserved Tyr-A731 might be able to form a

hydrogen bond with the phytol ester carbonyl oxygen of P_A. As the single amino acid deviations mentioned above are the only obvious differences between the different species, site-directed mutagenesis has been applied to clarify whether these differences are responsible for the spectroscopic peculiarities of the species. For *T. elongatus*, it has not been achieved to perform site-directed mutagenesis whereas such a system is established for *C. reinhardtii* and this organism has been preferred as a model organism for the analysis of photosynthesis using (site-directed) mutagenesis (12, 17–19). *C. reinhardtii* is able to grow heterotrophically on media with acetate as the carbon source (20) and is easily amenable to genetic manipulation with the advent of chloroplast genome transformation and selectable markers. Site-directed mutagenesis in turn is a powerful tool to identify the role of individual amino acids and to study the relationships between structure and function of photosynthetic reaction centers.

To get reliable information on species-specific differences, we measured and compared triplet-minus-singlet (T-S) difference, (P700⁺–P700) absorbance difference, and CD difference spectra of PS I core complexes from various species all purified using β -dodecyl maltoside as detergent. To study the influence of the amino acid side chains described above on the spectroscopic properties of P700 and to gain further insight into protein-cofactor interactions, we mutated Trp-A679 to Ala, Tyr, and His, Tyr-B659 to Trp, Leu, Ala, and His, and Tyr-A731 to His in *C. reinhardtii*. The effects of these mutations were analyzed using steady state and transient absorbance difference spectroscopy. Additionally, we applied redox titrations and electron nuclear double resonance (ENDOR) spectroscopy.

MATERIALS AND METHODS

Strains, Chloroplast Transformation, and Growth Conditions—As the recipient of the donor plasmids, strain *C. reinhardtii* CC2696 was used which in contrast to wild type carries the DS-521 nuclear mutation leading to a deficiency in the Cab proteins and a deletion in *psbA* causing the loss of PS II. Therefore, this strain is well suited for the preparation and analysis of PS I core complexes.

Chloroplast transformation and selection of the transformants on Tris acetate-phosphate plates containing 150 μ g/ml spectinomycin were carried out as described previously (17).

For enzyme purification, strains were grown heterotrophically in Tris acetate-phosphate and high salt medium/acetate medium (20) at 26 °C under low light conditions and supplemented with spectinomycin for mutant strains.

Site-directed Mutagenesis—Site-directed mutagenesis was performed according to the altered sites mutagenesis procedure (Promega, Heidelberg, Germany) on *psaA*-3 and *psaB*. Following mutagenesis and sequencing, a *Cla*I-*Pst*I fragment of *psaA*-3 was subcloned into pKR154 (17, 21) and reintroduced into *C. reinhardtii* CC2696. Plasmid pG528G, which was used for the reintroduction of *psaB*, has been described before (22). For mutations in *psaB*, the *Eco*RI-*Pst*I fragment that encodes the *psaB* gene and part of *rbcl* was subcloned into pAlter-1 to perform site-directed mutagenesis.

Preparation of PS I Core Complexes—Isolation of native and mutated PS I core complexes from *C. reinhardtii* CC2696 was performed according to Witt *et al.* (17) and from *S. oleracea* (spinach) as described by van der Lee *et al.* (23). The trimeric PS I core complexes from *S. platensis* have been prepared as described in Kruij *et al.* (24), from *T. elongatus* as described by Fromme and Witt (25) and from *Synechocystis* PCC 6803 (kind gift of M. Rögner) as described in Kruij *et al.* (26).

The Chl/P700 ratio has been determined for all PS I core complexes from all the species used in this work. It was calculated from the maximum flash-induced absorbance decrease in the *Q_y* region due to photo-oxidation of P700 by using the molar extinction difference coefficients given under “Results” and from the flash-induced absorbance increase at 826 nm due to the formation of P700⁺ using an extinction coefficient of 7500 M⁻¹ cm⁻¹. For all PS I core complexes from all the species, the ratio is 100 \pm 15. For the PS I preparations from *C. reinhardtii* and spinach, this gives evidence that virtually no LHC I is present bearing in mind that the Chl *a*/P700 ratio for PS I holocomplexes is about 200–250.

After purification the native and mutated PS I core complexes from

C. reinhardtii CC2696 were characterized by SDS-PAGE and Western blot analyses in comparison to the PS I holocomplex isolated from *C. reinhardtii* CC125 where LHC I is still present. The same amount of native and mutated PS I from CC2696 and wild type PS I from CC125 was loaded in each lane of a gel, and Western blot analysis with antibodies directed against PsaF showed that PsaF is present at the same level in the purified PS I complexes (not shown). Western blot analysis performed with antibodies directed against PsaA, -C, and -D demonstrated the existence of these subunits. For the native and mutated PS I preparations from CC2696, a minor contamination by LHC I can be deduced both from the measured Chl *a/b* ratio of 15 \pm 5 and from the Western blotting with antibodies directed against LHCI proteins. Chlorophyll concentrations were determined according to Porra *et al.* (27).

Transient Absorption Spectroscopy—Flash-induced absorbance difference spectra of (P700⁺–P700) were measured at room temperature as described previously (17) with PS I complexes diluted to 10 μ M Chl in 20 mM Tricine (pH 7.5), 25 mM MgCl₂, 100 mM KCl, 0.02% β -DM, 5 mM ascorbate, and 10 μ M phenazine methosulfate. The difference between the molar extinction coefficients of P700⁺ and P700 at the peak wavelength was calculated from the flash-induced absorption change of *N,N,N',N'*-tetramethyl-*p*-phenylenediamine dihydrochloride (TMPD) according to Hiyama and Ke (15). TMPD is oxidized by the flash-induced P700⁺. An extinction coefficient of 12,000 M⁻¹ cm⁻¹ has been determined for oxidized TMPD (pH 8.0).

For the light-minus-dark absorbance difference spectra at 77 K, PS I core complexes were diluted to 10 μ M Chl in 20 mM Tricine (pH 7.5), 25 mM MgCl₂, 0.02% β -DM, 5 mM ascorbate, and 60% glycerol. Measurements were performed as described previously (17).

To study the triplet state of P700, flash-induced T-S spectra have been recorded at 5 K. PS I core complexes were diluted to 10–15 μ M Chl in 100 mM CAPS (pH 10), 10 mM MgCl₂, 10 mM CaCl₂, and 0.02% β -DM. Glycerol was added to a final concentration of 65% (v/v). 10–20 mM dithionite was added to this solution under argon. The samples were then illuminated at 270 K for 3 min with a 250-watt focused tungsten lamp filtered by water and additional heat-absorbing filters. This procedure leads to the pre-reduction of the secondary electron acceptor A₁ whereby further electron transfer to A₁ is blocked. The primary radical pair P700⁺A₀⁻ formed under these conditions recombines with a high yield to the triplet state of P700. Measurements were performed according to Ref. 28.

Circular Dichroism—CD spectra were recorded on a Jasco J-720 spectrometer at room temperature as described previously (17). PS I complexes were diluted to 13 μ M Chl in 20 mM Tricine (pH 7.5), 25 mM MgCl₂, 100 mM KCl, 0.02% DM. For the measurements the solution was divided into two samples. Ferricyanide (1 mM) was added to one sample to oxidize P700, whereas 5 mM ascorbate and 10 μ M phenazine methosulfate was added to the second sample to keep P700 in the reduced state. Spectra of the samples with P700 oxidized or reduced were measured alternating. Oxidized-minus-reduced difference spectra were obtained by subtracting the average reduced from the average oxidized spectrum.

Redox Titration—To determine the oxidation midpoint potential of P700, the flash-induced absorbance change at 826 nm, associated with oxidation of P700, was measured as a function of the redox potential. Purified PS I complexes were diluted to 20–30 μ M Chl in 20 mM Tricine (pH 7.5), 100 mM KCl, 25 mM MgCl₂, 0.02% β -DM, and the redox potentials were adjusted by adding ferricyanide and ferrocyanide. After each experiment, the potential was measured using a combination Pt/Ag/AgCl electrode (Schott PT5900A) which was calibrated against the redox potential of a saturated solution of quinhydrone as a function of pH. A pH-meter (Knick PHM82) was used to read out the redox potential. All redox potentials are given relative to the standard hydrogen electrode (normal hydrogen electrode).

ENDOR—ENDOR measurements were performed on a Bruker ESP 300E X-band EPR spectrometer with home-built ENDOR accessories (29). ENDOR experiments were carried out on the cation radical P700⁺ of PS I complexes in frozen solution at 150 K as described earlier (17). Samples contained between 3 and 5 mM Chl. P700⁺ was generated by continuous illumination at room temperature with two 150-watt halogen lamps equipped with a water filter (2-cm path length) and a 700-nm edge filter for 20 s followed by rapid freezing under illumination.

ADMR Spectroscopy of the P700 Triplet State—Measurements were performed on thylakoid membranes that were diluted to 0.1 mM Chl in 100 mM CAPS (pH 10), 10 mM MgCl₂, 10 mM CaCl₂. Oxygen was removed using a glucose/glucose oxidase system, and 20 mM dithionite was added under nitrogen. Glycerol was added to a final concentration of 60% (v/v). The procedure for the pre-reduction of the secondary

electron acceptor A_1 was essentially the same as described for the flash-induced T-S spectra. Measurements were performed at 1.8 K. The absorption-detected magnetic resonance and the T-S microwave-induced spectra were recorded using the laboratory-built apparatus described previously (30).

RESULTS

By applying standard site-directed mutagenesis techniques, we constructed several mutants in PsaA and PsaB of PS I from *C. reinhardtii* CC2696 to investigate the influence of Trp-A679 and Tyr-B659 on the properties of P700. No PS I could be detected in mutants where Tyr-B659 was replaced by Trp or Leu. This is very surprising for the Trp mutant because all other species have a Trp at this position. The native and the mutated PS I core complexes WA A679, WH A679, WY A679, YA B659, and YH B659 from *C. reinhardtii* were purified and spectroscopically characterized together with PS I core complexes from four other species (*T. elongatus*, *S. platensis*, *Synechocystis* sp. PCC 6803, and *S. oleracea*) by steady state and transient absorption spectroscopy, circular dichroism, ADMR, ENDOR, and redox titrations.

Mutant Phenotype—As the mutations were introduced into the *Chlamydomonas* strain CC2696, which in contrast to wild type contains the DS-521 nuclear mutation leading to a deficiency in the Cab proteins and a deletion in *psbA* causing the loss of PS II, PS I is the main chlorophyll-binding protein. It is therefore possible to detect consequences of the amino acid substitution on the amount of PS I by inspection of the phenotype. All mutants contain PS I amounts comparable with the native CC2696 except for YW B659 and YL B659 which show a yellow phenotype indicating the absence of PS I. The negative phenotype of YW B659 was confirmed by Western blots (not shown) using thylakoid membranes and antibodies directed against PsaA which did not show any detectable amount of PS I.

Triplet-minus-Singlet (T-S) Absorbance Difference Spectra—To study the triplet state of P700, measurements were performed with PS I complexes under reducing conditions with the secondary acceptor A_1 in the reduced state. Therefore, the electron transfer to A_1 is blocked and the primary radical pair, $P700^+ A_0^-$, recombines to the triplet state of P700 with high yield. Fig. 2, A and B, shows the flash-induced T-S absorbance difference spectra of *C. reinhardtii*, *T. elongatus*, *S. platensis*, *Synechocystis*, and *S. oleracea* (spinach) detected at 5 K. These spectra reflect the absorbance difference between P700 in its triplet state and its singlet ground state. The spectra have been normalized between 660 and 726 nm to the same area assuming that the loss of oscillator strength upon triplet formation of P700 is the same in all species. The flash-induced absorbance difference spectra at 5 K attributed to 3P700 formation are virtually identical with the microwave-induced T-S spectra detected at 1.8 K (see Figs. 2A and 3A for *C. reinhardtii*; Schlodder *et al.* (28) for *T. elongatus*; and Fig. 2A and Carbonera *et al.* (30) for spinach). The same holds for *Synechocystis* and *S. platensis* (not shown). Because virtually identical T-S spectra of P700 are observed by both methods (flash-induced absorbance difference spectroscopy and ADMR), contributions of Chl triplets in the antenna can be excluded, except for the case when the resonance microwave frequency and the decay kinetics are identical for 3P700 and 3Chl . Despite some remarkable differences, all T-S spectra exhibit the following characteristic fingerprint-like features as follows: 1) a main bleaching around 700 nm, which is assigned to the disappearance of the low energy excitonic band of P700; 2) a second bleaching around 687 nm; and 3) positive bands around 682 and 672 nm. However, the spectra reveal some differences between the different species. The position of the main bleaching varies between 698 nm for *C. reinhardtii*, 701 nm for *T. elongatus*,

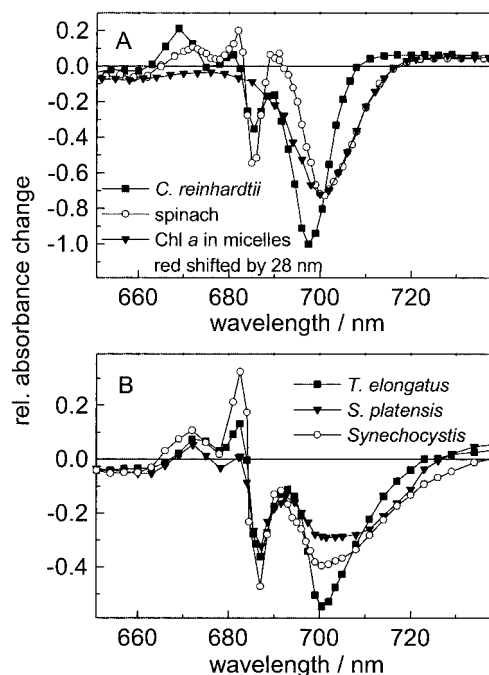


FIG. 2. Triplet-minus-singlet spectra of P700 from *C. reinhardtii* CC2696 and *S. oleracea* (A) and *T. elongatus*, *S. platensis*, and *Synechocystis* PCC 6803 (B) measured by flash-induced absorbance changes attributed to 3P700 formation, $T = 5$ K. For experimental details see "Materials and Methods." A, the T-S spectrum of Chl *a* in β -DM micelles is presented for comparison. It has been shifted to the red by 28 nm to align the main bleaching with the one of the ($^3P700-P700$) spectrum from spinach.

Synechocystis, and spinach, and 705 nm for *S. platensis*. It should be noted that the T-S spectrum of P700 measured with wild type PS I holocomplexes from *C. reinhardtii* CC125 also exhibits the main bleaching band at 698 nm. Even more impressive is the variation of the line shape of the low energy exciton band (compare the T-S spectra of *C. reinhardtii* and those of *Synechocystis* and *S. platensis*). For PS I from cyanobacteria the line width of the main bleaching band is broader, and the zero-crossing is shifted much more to the red (up to 735 nm for *Synechocystis*) compared with the green algae. The positive and negative features at the short wavelength side of the main bleaching band (687 nm (-), 682 (+), and 672 nm (+)) are differently pronounced for the species presented. It should be noted that the features in this spectral region are sensitive to the isolation procedure, pH values, and pretreatment (30).² The positive and negative band on the blue side of the main bleaching are blue-shifted for the green algae by 2–3 nm compared with the other species.

For comparison, we have measured the T-S spectrum of monomeric Chl *a* in β -DM micelles using the same apparatus. In Fig. 2A we plotted the spectrum, shifted to the red by 28 nm to align the peak with the one of the ($^3P700-P700$) spectrum from spinach. It should be noted that the large line width of the Q_y band of the monomeric Chl *a*, which is bleached upon triplet formation, is mainly due to inhomogeneous broadening (31), whereas the low energy exciton band of P700 is predominantly homogeneously broadened (16, 32). The T-S spectrum of Chl *a* completely lacks the second sharp negative and positive features at shorter wavelengths. Excitonic interactions between the six Chls in the reaction center can probably account for these additional spectral features (see under "Discussion").

The effects of the replacement of Tyr B659, Trp-A679, and

² E. Bordignon, D. Carbonera, and E. Schlodder, unpublished results.

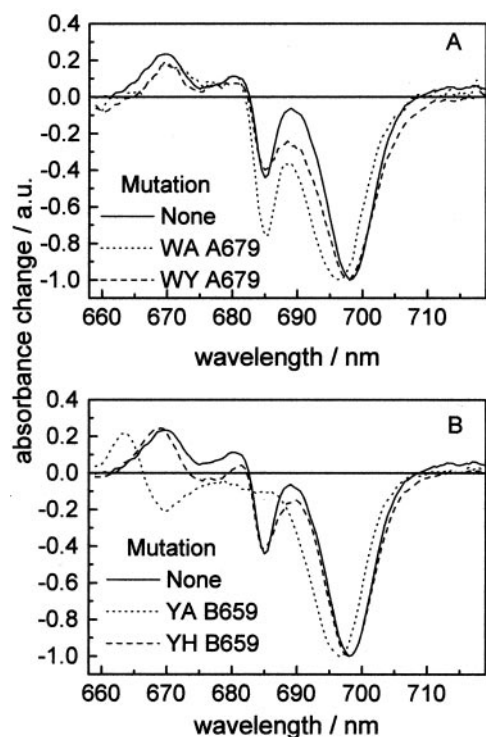


FIG. 3. ADMR measurements of triplet-minus-singlet spectra of P700 of native and mutated PS I from *C. reinhardtii* CC2696 WA A679 and WY A679 (A), and YA B659 and YH B659 (B), taken at the maximum of the intensity of the $|D|-|E|$ transitions: 718.5 MHz (WT), 728.7 MHz (WA A679), 719 MHz (WY A679), 718.5 MHz (YA B659), and 716.5 MHz (YH B659). The modulation frequency was 33 Hz, the microwave power 800 milliwatts, the optical resolution 1.5 nm, and $T = 1.8$ K. For experimental details see "Materials and Methods."

Tyr-A731 have been monitored by ADMR-detected T-S spectra. Fig. 3, A and B, shows the T-S absorbance difference spectra of native and mutated PS I from *C. reinhardtii* CC2696. The spectra are normalized to -1 at the minimum of the main bleaching band to allow better comparison. The position of the main bleaching band is blue-shifted by about 2 nm for the mutant WA A679 and the second bleaching at about 685 nm is slightly more pronounced compared with native PS I. The T-S spectrum for the mutant WY A679 is essentially the same as that of unmutated PS I (Fig. 3A). The main bleaching of YA B659 is blue-shifted by about 2 nm, and the second negative bleaching is completely absent in this mutant. Moreover, the positive band located at 670 nm in the unmutated PS I is blue-shifted to 665 nm for the mutant YA B659, whereas a negative band is appearing at 670 nm (Fig. 3B). The spectrum for YH B659 is essentially unchanged compared with native PS I (Fig. 3B).

The zero field-splitting (ZFS) parameters $|D|$ and $|E|$ reflect the energy splitting between the triplet sublevels in a zero magnetic field. The ZFS parameter depend on the spatial distribution of the unpaired electrons in the triplet state over the chlorophylls P_A and P_B , and/or on the admixture of charge-transfer states. At low temperature ($T = 1.8$ K) the ZFS parameters of 3P700 for the mutants are almost unchanged in comparison to unmutated PS I (not shown). They are virtually identical to those of triplet states from monomeric Chl a (33, 34) or Chl a'^3 in organic solvents. This has been taken as evidence that the triplet state of P700 is mainly localized on one of the chlorophylls constituting P700. The

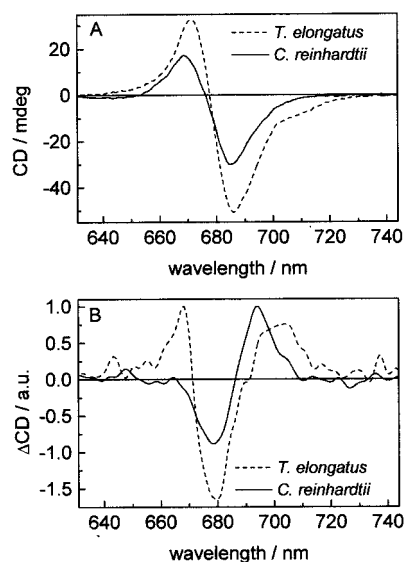


FIG. 4. A, CD spectra of PS I with P700 in the oxidized form; B, ($P700^+-P700$) circular dichroism spectra of PS I core complexes from *C. reinhardtii* CC2696 and *T. elongatus* measured at room temperature with a spectral bandwidth of 2 nm. The difference spectra were obtained by subtracting the CD spectra measured with P700 in the reduced state from those measured with P700 in the oxidized state. Oxidation was achieved with 1 mM ferricyanide. The difference spectra are normalized to 1 at the positive maximum to allow better comparison. The absolute ΔCD values for *C. reinhardtii* are 2.1 millidegrees (OD_{677nm} 1.1) and for *T. elongatus* 3.8 millidegrees ($OD_{678.5nm}$ 1.1) at the positive maximum.

localization of the triplet state is thus not significantly altered in the mutants.

($P700^+-P700$) CD Difference Spectra at Room Temperature—The CD spectra of PS I core complexes from *C. reinhardtii* CC2696 and *T. elongatus* with P700 in the oxidized form are shown in Fig. 4A. In accordance with CD spectra of PS I complexes reported earlier in the literature (23, 35-37), the rotational strength of the positive band on the high energy side is smaller than that of the negative band on the low energy side. The CD spectrum of *C. reinhardtii* displays the negative band at 685 nm and the positive band at 669 nm, whereas the one of *T. elongatus* has its negative band at 686 nm and the positive band at 671 nm. In addition, a broad negative absorption is observed between 700 and 720 nm for the cyanobacterium which can be attributed to the long wavelength Chls. The excitonic interactions between all chlorophylls of PS I contribute predominantly to the CD intensity, although the unequal rotational strength of both bands (non-conservative spectra) clearly indicates other contributions.

In order to obtain information on the excitonic coupling between the chlorophylls constituting the primary donor in PS I, the ($P700^+-P700$) circular dichroism difference spectra were recorded (see Fig. 4B). The ΔCD spectra have been normalized to 1 at the positive maximum to allow a better comparison.

In *C. reinhardtii*, the ΔCD spectrum is dominated by two components located at 694 (positive rotational strength) and 678 nm (negative rotational strength). In *T. elongatus*, we observe a band of negative rotational strength at 679 nm and two bands of positive rotational strength at 668 nm and at about 702 nm.

In order to monitor changes of the excitonic coupling between the reaction center Chls induced by the mutations in *C. reinhardtii*, ($P700^+-P700$) circular dichroism difference spectra were recorded. The spectra for native PS I and PS I containing the mutations WA A679 and YA B659 are shown in Fig. 5. The spectrum of WA A679 is blue-shifted by 2–3 nm compared with

³ F. Lenzian, L. Fiedor, and W. Lubitz, unpublished results.

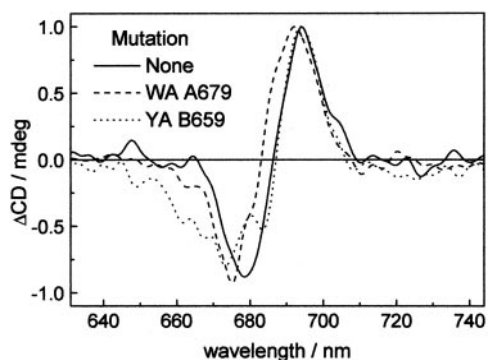


FIG. 5. (P700⁺-P700) circular dichroism spectra of native and mutated (WA A679 and YA B659) PS I complexes from *C. reinhardtii* CC2696 measured at room temperature with a spectral bandwidth of 2 nm. The spectra were obtained by subtracting the CD spectra measured with P700 in the reduced state from those measured with P700 in the oxidized state. Oxidation was achieved with 1 mM ferricyanide. The spectra are normalized to 1 at the positive maximum to allow better comparison. The absolute CD values are 2.1 millidegrees (native PS I; OD_{677nm} 1.1), 2 millidegrees (WA A679; OD_{677nm} 0.98), and 2.2 millidegrees (YA B659; OD_{676nm} 1.1).

unmutated PS I. For YA B659, the shape and position of the band with the positive rotational strength is similar to unmutated PS I, whereas the one with negative rotational strength is slightly shifted. The CD difference spectrum of YH A731 is nearly the same as that of native PS I (not shown).

(P700⁺-P700) Absorbance Difference Spectra at Room Temperature and 77 K—The optical features of the primary electron donor were additionally investigated by recording oxidized-minus-reduced absorbance difference spectra. The absorbance changes due to the oxidation of P700 were monitored as a function of wavelength. The molar extinction difference coefficient for the maximum bleaching in the *Q_y* region has been measured as described by Hiyama and Ke (15). The values are 61,000 M⁻¹ cm⁻¹ for *T. elongatus* and 57,000 M⁻¹ cm⁻¹ for *Synechocystis*, 83,000 M⁻¹ cm⁻¹ for *S. platensis*, and 64,000 M⁻¹ cm⁻¹ for spinach. For *C. reinhardtii* the following molar extinction difference coefficients have been determined: 100,000 M⁻¹ cm⁻¹ for native PS I, 73,000 M⁻¹ cm⁻¹ for WA A679, 98,000 M⁻¹ cm⁻¹ for YA B659, 88,000 M⁻¹ cm⁻¹ for YH A731, and 90,000 M⁻¹ cm⁻¹ for YH B659. The margin of error is about 5%.

The (P700⁺-P700) spectra in the *Q_y* region obtained for *C. reinhardtii*, *T. elongatus*, *Synechocystis*, spinach, and *S. platensis* at room temperature are shown in Fig. 6A. Although the overall shape of the spectra displaying one main bleaching band and a second smaller negative band seems to be similar, several differences between the spectra from different species can be observed. The main bleaching band of *C. reinhardtii* is located at 698 nm which is the furthest to the blue. The position of the main bleaching band is at 702 nm for *Synechocystis* and at 703 nm for *T. elongatus*, *S. platensis*, and spinach. A second smaller bleaching band appears for all species besides the green algae where it is only visible as a shoulder at about 682 nm. The positions of this band (-) and of a positive band (+) between the two bleachings are 682 (-) and 691 nm (+) for *T. elongatus*, 677.5 (-) and 687.5 nm (+) for *Synechocystis*, 682 (-) and 688 (+) for *S. platensis*, and 685 (-) and 691 (+) for spinach. For *Synechocystis* the positive band even exceeds the zero line and reaches positive values. Another difference is the zero crossing in the red region at 725 nm for *C. reinhardtii*, at 728 nm for spinach, at about 730 nm for *S. platensis* and *T. elongatus*, and at 738 nm for *Synechocystis*. In the Soret region, the position of the main bleaching band is at about 431 nm for *C. reinhardtii* and at about 434 nm for *T. elongatus* and *S. platensis* (Fig. 6B).

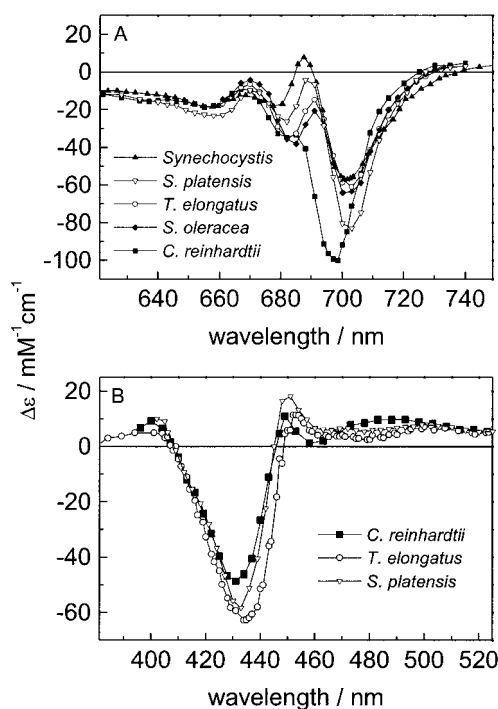


FIG. 6. Flash-induced (P700⁺-P700) absorbance spectra of PS I complexes from *C. reinhardtii* CC2696, *T. elongatus*, *Synechocystis* PCC 6803, *S. platensis*, and *S. oleracea* measured at room temperature. A, *Q_y* region. B, Soret region. Samples were excited with saturating flashes of about 15 μs in duration from a xenon flash lamp. For experimental details see "Materials and Methods."

The room temperature (P700⁺-P700) spectra of mutated and native PS I from *C. reinhardtii* CC2696 are compared in Fig. 7. A blue shift of about 2–3 nm of the main bleaching band is observed for WA A679 coupled with a decrease of the oscillatory strength of this band, whereas the oscillatory strength of the band at 682 nm increases (Fig. 7A). For YA B659 the main bleaching band is also shifted to blue by about 2–3 nm and a rather broad additional bleaching is observed between 665 and 685 nm (Fig. 7B). A slight blue shift can also be seen for the mutant YH B659, and the molar extinction difference coefficient is slightly reduced.

The (P700⁺-P700) spectra detected at 77 K are presented in Fig. 8. These spectra were obtained by subtracting the absorbance spectra of PS I in the dark adapted state (with P700 reduced) from those after illumination. After illumination by saturating flashes from a xenon flash lamp, an irreversible charge separation P700⁺F_{AB}⁻ is induced at 77 K in a fraction of the PS I complexes (38, 39). The size of this fraction varies between the different organisms (not shown). The spectra exhibit strong contributions from electrochromic bandshifts induced by the positive charge localized on the oxidized P700. All spectra have been normalized to -1 at the minimum of the long wavelength bleaching band. The spectra for *C. reinhardtii*, *T. elongatus*, *S. platensis*, *Synechocystis*, and spinach are shown in Fig. 8, A and B. The spectrum of *C. reinhardtii* is dominated by a strong bleaching at 700 nm and a strong absorbance increase at 689 nm. Minor absorbance difference bands are observed at 683 (-), 670 (+), and 660 (-) nm. The spectra of the other species display the following features: 702 (-), 689 (+), 684.8 (-), 677.9 (+), 672.8 (-), and 667.9 (+) nm for spinach; 703 (-), 698.2 (+), 696.5 (-), 690.2 (+), 684.4 (-), 680.8 (+), 679.6 (-), 677.6 (+), 674 (-), and 669.4 (+) nm for *T. elongatus*; 701.3 (-), 694.7 (+), 689.3 (+), 683.1 (-), 678.1 (+), 673.7 (-), and 667.5 (+) nm for *Synechocystis*; and 704.3 (-), 691.1 (+), 682.9 (-), and 669 (+) nm for *S. platensis* (+/-)

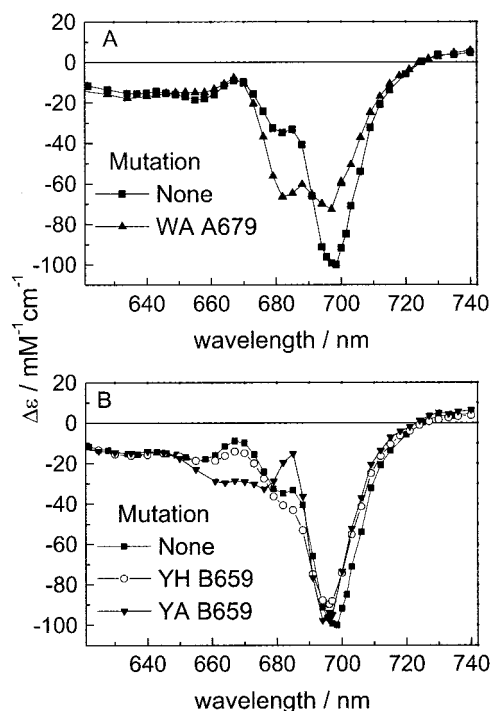


FIG. 7. Flash-induced ($P700^+ - P700$) absorbance difference spectra of native and mutated PS I core complexes from *C. reinhardtii* CC2696 measured at room temperature. A, WA A679; B, YA B659 and YH B659. Samples were excited with saturating flashes of about 15 μ s in duration from a xenon flash lamp. For experimental details see "Materials and Methods."

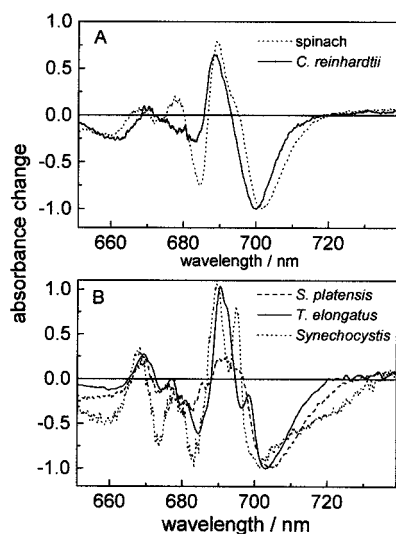


FIG. 8. Light-minus-dark-difference spectra of PS I complexes from *C. reinhardtii* CC2696 and *S. oleracea* (A) and *T. elongatus*, *Synechocystis* PCC 6803, and *S. platensis* (B) at 77 K. The curves were obtained by subtracting the absorbance spectra in the dark-adapted state from those after illumination with 30 saturating xenon flashes. The spectra are normalized to -1 at the negative maximum. Spectra were recorded with data intervals of 0.1 nm, a scan speed of 20 nm/min, and a spectral bandwidth of 1 nm. For details see "Materials and Methods."

indicates an absorbance increase or decrease induced by the oxidation of P700, respectively).

The ($P700^+ - P700$) spectra at 77 K of native and mutated PS I from *C. reinhardtii* CC2696 are shown in Fig. 9, A and B. The difference spectrum of the native PS I has been described before (Fig. 8A). For the mutant WA A679, the main bleaching band is blue-shifted to 696 nm, whereas the strong positive

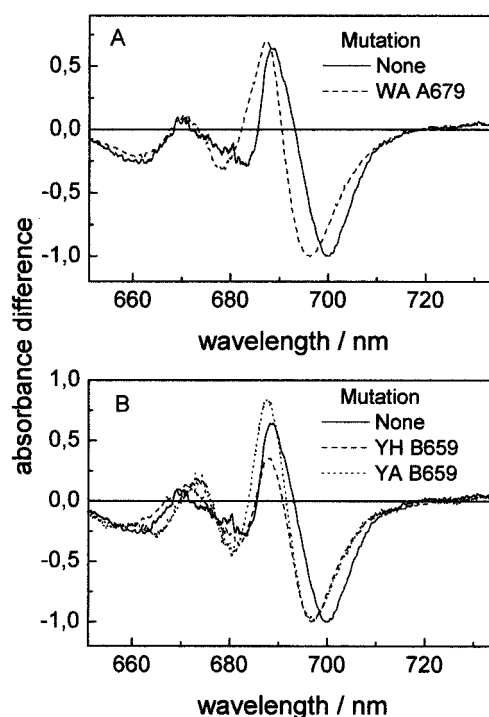


FIG. 9. Light-minus-dark-difference spectra of native and mutated PS I complexes from *C. reinhardtii* CC2696 measured at 77 K. A, WA A679; B, YA B659 and YH B659. The curves were obtained by subtracting the absorbance spectra in the dark-adapted state from those after illumination with 30 saturating xenon flashes. The spectra are normalized to -1 at the negative maximum. Spectra were recorded with data intervals of 0.1 nm, a scan speed of 20 nm/min, and a spectral bandwidth of 1 nm. For details see "Materials and Methods."

band is shifted 2 nm to the blue (Fig. 9A). The absorbance difference band at 670 nm remains unchanged, whereas this band is red-shifted by about 4 nm in the mutant YA B659. The main bleaching band of YA B659 is displaced 3 nm to the blue shift and the strong positive absorbance difference band is located at 688 nm (Fig. 9B). For the mutant YH B659, the main bleaching band is blue-shifted to 697 nm, whereas the two positive bands are only slightly affected.

Oxidation Midpoint Potential of $P700^+ / P700$ —The midpoint potential (E_m) of $P700^+ / P700$ is a very sensitive probe for changes of the environment of the primary donor. To determine the oxidation midpoint potential of P700, the flash-induced absorbance change at 826 nm, associated with the oxidation of P700, was measured as a function of the potential adjusted by adding varying amounts of ferricyanide and ferrocyanide. The dependence of the amplitude of the absorbance change could be satisfactorily fitted using the one-electron Nernst equation. In comparison to *C. reinhardtii*, the midpoint potentials of $P700^+ / P700$ are decreased for the cyanobacteria, whereas that for spinach is increased (see Table I, last column). The midpoint potentials of $P700^+ / P700$ of the mutants WA A679, WY A679, and YA B659 remain unchanged within the error limit. In contrast, the midpoint potential of $P700^+ / P700$ is decreased for YH B659, whereas the one of WH A679 is slightly lowered. The error limits for the ΔE_m values obtained by one set of measurements under identical conditions are about ± 4 mV corresponding to the standard deviation derived from the fits. The absolute value for native PS I from *C. reinhardtii* CC2696 was determined to 478 ± 8 mV. In this case the error includes additionally the uncertainty of the calibration of the electrode. It should be noted that the midpoint potential of $P700^+ / P700$ determined with wild type PS I holocomplexes from *C. reinhardtii* CC125 is the same within the limits of error.

TABLE I
Hyperfine couplings of the methyl protons (A_{iso}) in MHz of P700⁺ of native and mutated PS I from *C. reinhardtii* CC2696 and in comparison the hfc of PS I from other species and Chl a^{++} Oxidation midpoint potential of P700⁺/P700. ND, not done.

	Methyl group			ΔE_m (mV) ^a
	12	7	2	
Native	5.3	3.7	2.9	0
WA A679	5.4	3.4	2.9	+4
WH A679	5.4	3.5	2.7	-8
WY A679	5.2	3.4	3.0	+2
YA B659	6.0	3.9	2.8	+4
YH B659	5.6	3.7	2.9	-26
<i>T. elongatus</i> ^b	5.3	3.5	2.9	-39
<i>Synechocystis</i> ^b	5.6	3.6	2.9	-15
Spinach ^b	5.6	3.6	2.9	+17
<i>S. platensis</i>	ND	ND	ND	-48
Chl a^{++c}	7.1	3.0	3.0	ND

^a ΔE_m is the difference $E_m - E_{m(\text{native})}$. The absolute value for the oxidation midpoint potential for P700 of native PS I from *C. reinhardtii* was determined to be $E_{m(\text{native})} = (478 \pm 8)$ mV.

^b Values have been taken from Ref. 11.

^c The values of Chl a^{++} in $\text{CH}_2\text{Cl}_2/\text{THF}$ are taken from Ref. 50. The error in the hfc is ± 0.1 MHz for the methyl groups. The A_{iso} values have been calculated from the A_{\parallel} and A_{\perp} components with the equation $A_{\text{iso}} = 1/3(A_{\parallel} + 2A_{\perp})$.

ENDOR—ENDOR spectroscopy was used to characterize the electronic structure of P700⁺ by resolving the individual proton hyperfine couplings (hfc). The assignment of the obtained hfc to specific hydrogens of P700 was based on the comparison with ENDOR data reported earlier for Chl a^{++} in organic solvents and P700⁺ in PS I single crystals (13). Käss *et al.* (13) concluded from EPR/ENDOR experiments that the spin density is mainly localized ($\geq 85\%$) on one of the Chls constituting P700.

The isotropic hyperfine couplings extracted from the spectra of native and mutated PS I from *C. reinhardtii* CC2696 in frozen solution (not shown) are summarized in Table I. For comparison, the proton hfc of Chl a^{++} measured in organic solvents are given. On the basis of the analysis of ENDOR spectra of P700⁺ obtained in PS I single crystals, the second largest splittings (line pairs 12) belong to the CH_3 protons at position 12 of the chlorine ring (13). The ENDOR line pairs at about 3.6 and 2.9 MHz were assigned to the protons of the two methyl groups at positions 7 and 2. These resolved hfc (see Table I) belong to the spin carrying Chl, P_B.

In comparison to the unmutated PS I, the hfc of the methyl protons at position 12 of the spin carrying Chl P_B is increased for YA B659 by about 0.7 MHz (Table I), for the methyl group at position 7 by about 0.2 MHz, whereas the hfc of the methyl group at position 2 is even slightly decreased. For YH B659 the hfc of the methyl protons at position 12 are slightly increased by about 0.3 MHz, whereas there is no significant change of the hfc for the methyl groups at positions 7 and 2. For the mutants WA A679, WH A679, and WY A679, the changes of the hfc of the methyl protons at position 12 of the spin carrying Chl P_B is close to the error limit. In contrast, the hfc of the methyl group at position 7 is decreased between 0.2 and 0.3 MHz for these mutants (Table I), whereas hardly any effect on the methyl group at position 2 is observed besides for WH A679 where this value is slightly decreased. The hfc of the methyl groups at positions 2 and 7 are very similar for *C. reinhardtii*, *Synechocystis*, spinach, and *T. elongatus*. This also holds for the hfc of the methyl protons at position 12 of *C. reinhardtii* and *T. elongatus*. Only the hfc of the methyl protons at position 12 of *Synechocystis* and spinach are slightly increased. Up to now, we are not able to resolve any changes in the spectral region that has been discussed previously (13) to contain contributions

from the second Chl due to the small fraction of the spin localized on this side.

DISCUSSION

Species-specific Differences of Optical Properties of P700—To obtain reliable information on the spectroscopic properties of PS I from several species, we compared the flash-induced absorbance difference spectra of (P700⁺-P700) and of (³P700-P700) of PS I complexes from *C. reinhardtii*, *T. elongatus*, *Synechocystis* PCC 6803, *S. platensis*, and *S. oleracea* (spinach) measured under the same conditions. All PS I core complexes have been isolated using the mild detergent β -dodecyl maltoside. This is an important prerequisite as the spectra are also dependent on the purification procedure and the detergent used for the preparation (30, 40). Although common characteristic features exist for all species, significant differences can still be observed (Figs. 2, 6, and 8). They mainly concern the position and the line shape of the main bleaching band as well as the features around the second bleaching. Remarkably, the molar extinction difference coefficients for the maximum bleaching in the Q_y region in the (P700⁺-P700) spectra at room temperature (Fig. 6) have been found to vary considerably. In good approximation, the area under the curves in the Q_y region is the same for all species indicating that the loss of oscillator strength upon oxidation of P700 is virtually identical for all of them. Whereas the $\Delta\epsilon$ value of spinach and *T. elongatus* is in good agreement with the value of $64000 \text{ M}^{-1} \text{ cm}^{-1}$ (15) which is widely used in the literature for all species, it becomes evident that the $\Delta\epsilon$ value has to be determined for each PS I sample. It should be noted that this value also depends on the oligomeric state of the PS I complex (41) and on the preparation procedure and the detergent (not shown). The spectra obtained with PS I complexes of *C. reinhardtii* display the largest differences compared with the others as the position of the main bleaching band is the furthest to the blue, the extinction difference coefficient is the largest and the second bleaching is only visible as a shoulder. A blue shift of the main bleaching band is also visible in the Soret region for *C. reinhardtii*. The position of the main bleaching band in the Q_y region in the other four species is located between 701 and 703 nm with similar extinction difference coefficients besides *S. platensis* where this value is somewhat larger. Striking differences between the species are also observed for the position and shape of the smaller second bleaching at about 682 nm and the spectral region between the two bleachings (see Fig. 6). Only in *Synechocystis* is an absorbance increase observed between the two negative bands, and the whole feature is blue-shifted compared with the other species.

Lowering the temperature yields absorbance difference spectra that are better resolved due to the narrowing of the absorbance bands. On the other hand, electrochromic shifts of absorbance bands as a consequence of the formation of P700⁺ become more visible in the (P700⁺-P700) spectra upon lowering the temperature leading to additional narrow positive and negative bands. This can be explained in part by the fact that at low temperatures the shielding of the electric field is weakened due to the temperature dependence of the dielectric relaxation. The long range electrostatic interactions due to the charge on P700 may not only affect Chls in close proximity of P700 but very likely also those located in the core antenna system. The dominant absorbance increase at about 690 nm probably caused by an electrochromic bandshift is of comparable size as the absorbance decrease due to the bleaching of the low energy exciton band in all the species. The only exception is the PS I complex of *S. platensis*.

We also monitored T-S absorbance difference spectra of P700 at 5 K (Fig. 2). The main bleaching band can be assigned to the

disappearance of the low energy exciton band upon triplet formation whereby the excitonic interaction between the Chl carrying the triplet state and the neighboring Chls of the reaction center is lost. The spectra represent very likely pure absorbance difference spectra of the reaction center because contributions of electrochromic bandshifts are avoided upon formation of the triplet state of P700. As the T-S spectrum of monomeric Chl *a* in micelles lacks the narrow features on the short wavelength side of the main bleaching band, they probably reflect the altered excitonic interactions between the six reaction center Chls.

The (3 P700–P700) (Fig. 2) as well as the (P700 $^{+}$ –P700) absorbance difference spectra (Fig. 8) indicate that the low energy exciton band is very broad for all species even at low temperatures. A line width of 300 cm $^{-1}$ at 5 K has been determined by hole-burning experiments using PS I complexes from spinach (32). The low energy exciton band of P700 is predominantly homogeneously broadened whereas the large line width of the Q_y band of monomeric Chl *a* in micelles, which is bleached upon triplet formation, is mainly due to inhomogeneous broadening (31). The remarkable homogeneous broadening of the low energy exciton band has been explained by an unusually strong electron-phonon coupling probably due to mixing of excited states with charge transfer states. If the electronic transition involves a substantial displacement of charge, the protein environment reacts stronger on an excitation thereby giving rise to stronger vibrational side bands. Interestingly, the line width of the low energy exciton band of P700 in PS I from cyanobacteria is even larger than that in PS I from higher plants (see Fig. 8). In addition, the strongly red-shifted zero crossings for the cyanobacteria (708 nm for *C. reinhardtii* up to 740 nm for *Synechocystis*; see Fig. 2) strongly indicate that the 0 \rightarrow 0 transition energy is lowered in cyanobacteria. Taken together this means that the absorption of the primary donor extends much more to the red. Thereby the overlap between the P700 absorption and the fluorescence of the red Chls in the core antenna is enhanced and consequently the possibility of direct energy transfer from these red Chls to P700 itself. The 77 K absorption spectra of the PS I core complexes from all species under study (data not shown) show that all species contain red Chls absorbing between 705 and 708 nm whereby *C. reinhardtii* and spinach contain the smallest number of these red Chls. The trimeric PS I core complexes in cyanobacteria contain in addition Chls absorbing even further to the red at 714 (in *Synechocystis*), 719 (in *T. elongatus*), and 740 nm (in *S. platensis*) (42). Keeping this in mind, the presence of the broad and red-shifted low energy exciton transition in cyanobacteria might be of functional relevance increasing the efficiency of energy transfer from these far red antenna Chls to the reaction center. If antenna Chls are present, which are able to exploit the red region of the spectrum, the absorbance wavelength of the photochemical trap also has to be shifted to the red to facilitate the trapping of excitation energy localized on red chlorophylls present in the core antenna.

Interestingly, green algae and spinach, which possess their most red antenna Chls in the external LHCI complexes, do not display such a broad low energy exciton band. For these red Chls, the distance to P700 is too large for a direct energy transfer, *i.e.* the efficiency of trapping would not be increased if the absorption of the primary donor extends more to the red. The spectroscopic differences between the primary donor of PS I in cyanobacteria and that in green algae and higher plants are hard to explain keeping in mind that the amino acid residues in the vicinity of P700 are highly conserved and are even identical for *T. elongatus* and spinach. The differences could be

caused by long range effects due to variations of amino acids in PsaA and PsaB located further away that might slightly modify the geometrical arrangement of the cofactors, thus changing, for example, the charge transfer character of the excited state of the primary donor.

To get further insight into these species-specific differences, we investigated PS I complexes also with circular dichroism spectroscopy. For the interpretation of the various (P700 $^{+}$ –P700) CD difference spectra, it should be kept in mind that the spectral features cannot easily be explained by a model of an excitonically coupled dimer but, as has been shown before, that all excitonic interactions between the six reaction center Chls have to be taken into consideration (see Ref. 37 for the calculation of the excitonic couplings). This was shown by comparison of the measured with a calculated CD difference spectrum where only the excitonic interaction between P_A and P_B was considered (17). Moreover, the calculated CD difference spectrum taking into account the excitonic interactions between all six reaction center Chls (not shown) has the qualitative features of the measured one for *T. elongatus* (Fig. 4). Based on the measurement of the Δ CD of P700 in *S. platensis*, Karapetyan and co-workers (43) proposed that even contributions of antenna chlorophylls located closest to the reaction center are observed. Comparison of the CD difference spectra of *T. elongatus* and *C. reinhardtii* reveals several differences, and the spectrum for *C. reinhardtii* obviously cannot be simulated on the basis of the structural data of the cyanobacterium. This gives evidence that structural differences exist in the arrangement of the cofactors between the species, besides the fact that the amino acid sequence is highly conserved.

Effects of the Mutations on the Optical Properties of P700—The most challenging task is to clarify the origin of the species-specific differences. They seem to be quite surprising because it is generally assumed that the structures of PS I complexes from different species are rather similar. Furthermore, the amino acid sequences around the primary donor P700 are highly conserved with only few deviations. It has already been mentioned that in *C. reinhardtii* a Tyr is found at position B659 where a Trp is conserved in all other species. Another variation in the amino acid sequence is found in *Synechocystis* where in the homologous position in the A subunit A679 is a Phe instead of Trp present in the other species. To investigate whether these amino acid variations might be responsible for the spectroscopic differences, we constructed mutants at these two positions in *C. reinhardtii* CC2696. Furthermore, we assume that Tyr-B659 might be able to form a hydrogen bond to the keto group of the phytyl side chain of P_B. As Tyr-A731 present in all species is a putative hydrogen bond donor to the keto group of the phytyl side chain of P_A, we also constructed a mutant at this position⁴ to investigate further the influence of hydrogen bonds on P700 and to understand the influence of the protein environment on the cofactors in photosynthetic reaction centers. Although in this case the specific influence of the hydrogen bond might be negligible as the keto group of the phytyl side chain does not belong to the conjugated π -orbital system, it might play a role in stabilizing the position of the phytyl side chain with respect to the accessory Chls. It should be noted that the phytyl side chain of P_A is in close proximity to the accessory chlorophyll B_A, whereas the phytyl side chain of P_B is close to the accessory chlorophyll B_B (8), whereas the excitonic coupling is strong between P_A and B_B and P_B and B_A, respectively (37).

Strikingly, the mutant YW B659 shows a negative phenotype which seems to be quite surprising. Because a Trp is present in

⁴ H. Witt, unpublished data.

all other organisms, it is quite reasonable to assume a similar three-dimensional structure considering the conservation of the amino acid sequence around P700. However, Tyr-B659 cannot be replaced by Trp in *C. reinhardtii*. Probably the assembly is dramatically affected, and it can be assumed that there are steric constraints unique to this organism. It seems as if the side chain of Trp impedes the assembly of PS I. It is well known that PsaA and PsaB play a critical role in the assembly of PS I in *C. reinhardtii* and that complexes assembled only partially are rapidly degraded in this organism (44).

The effects of the mutations on the optical properties have been characterized by steady state and transient absorbance difference spectroscopy. Replacement of Trp-A679 and Tyr-B659 by Ala alter significantly the optical properties of the PS I reaction center (see Figs. 3, 5, 7, and 9). For both mutants, we observe a blue shift of the main bleaching band in the triplet-minus-singlet absorbance difference spectra and (P700⁺-P700) absorbance difference spectra at room temperature and 77 K. This also holds for WA A679 looking at the CD difference spectrum. The position of the main bleaching band is related to the strength of the excitonic coupling between the Chls of the dimer and the two accessory Chls. Therefore it can be assumed that the blue shift indicates a decrease of this excitonic interaction by the mutations. One reason for this might be that Ala destabilizes the protein due to the smaller size and a loss in hydrophobicity with respect to Tyr and Trp. In addition, removal of the aromatic π -systems in the surrounding of cofactors may impede the reorganization of the protein surrounding upon excitation which finally gives rise to higher site energies. As a consequence the low energy exciton band will also be blue-shifted. The spectral features between 660 and 690 nm are affected differently for both mutants. This spectral range very likely reflects excitonic interactions with other pigments in the reaction center and, in case of the (P700⁺-P700) spectra, electrochromic bandshifts of pigments in close proximity. For WA A679 the peak maximum of the main bleaching band is decreased, whereas the peak maximum of the second bleaching is increased. In the T-S spectrum of YA B659, the second bleaching is completely absent, whereas the positive band around 670 nm is blue-shifted. As Tyr-B659 seems to stabilize the phytyl side chain of P_B which is located in close proximity to the accessory Chl B_B, these changes can be reasonably explained if we assume that the spectral properties of B_B are altered due to structurally induced changes. The broad absorption between 665 and 685 nm in the (P700⁺-P700) absorbance difference spectrum of YA B659 gives additional evidence for the contribution of the B_B in this spectral region. As Trp-A679 might mainly affect P_A, a mutation will exert its effect on Chls nearby only indirectly via the excitonic coupling. P_A is excitonically coupled mainly with P_B and B_B, whereas the interaction of the dimer is reflected in the main bleaching band. So far, it is not known which spectral features represent the remaining interactions within the reaction center. It is therefore reasonable to assume that both mutations influence the interaction of P_A and B_B and that this interaction becomes at least partly visible in the second bleaching of the (T-S) absorbance difference spectra. Furthermore, there is strong evidence that the influence of the mutations induces not only changes in the excitonic interaction with accessory chlorophylls but that electrochromic bandshifts due to P700⁺ formation are altered.

The exchange of Tyr-B659 against His leads only to minor changes in the spectra which might indicate that, although the hydrogen bond is probably broken, this exchange is not destabilizing the protein scaffold to a larger extent. The same seems to be the case with the YH A731 mutant (not shown). By using the Swiss PdbViewer, we have estimated that the distance

between the histidine and the keto group of the phytyl side chain is more than 4 Å, *i.e.* too large to form a hydrogen bond.

Taken together the results give evidence that the few amino acid variations between the different species cannot account for all the differences between the spectral properties of P700 from higher plants, algae, and cyanobacteria.

Effects of the Mutations on the Redox Properties of P700⁺/P700—The redox potential is a measure for the energy difference between the neutral ground state and the oxidized state of P700. The energy of the oxidized state can be influenced by electrostatic effects like permanent dipoles, charges, and the polarizability of the surrounding residues. Hydrogen bonding in turn can stabilize the neutral ground state. The influence of hydrogen bonds on the oxidation midpoint potential has been demonstrated for the primary donor of PS I in *C. reinhardtii* (17) and for bacterial reaction centers (45). It should be noted that in these cases the carbonyl groups involved in the hydrogen bonding interaction were part of the conjugated π -system.

Tyr-A731 and Tyr-B659 are putative hydrogen bond donors to the keto groups of the phytyl side chain of P_A and P_B, respectively. Substitution of Tyr-B659 by His leads to a decrease of the oxidation midpoint potential of P700⁺/P700 (a similar effect is observed for Tyr-A731, not shown), but the redox potential remains unchanged in the mutant YA B659. Since in both cases the hydrogen bond has probably been broken, the results indicate that the effects cannot be correlated with a specific influence of the hydrogen bond; this was the case after the hydrogen bond to the 13¹ keto group of P_A had been removed. A possible explanation is that the keto groups of the phytyl side chains are not part of the conjugated π -system. However, it seems more likely that the histidine in close proximity exerts an influence on P700. A slight diminution of the midpoint potential was also observed for WH A679 where no hydrogen bond has been removed.

Distribution of the Electron Spin in P700⁺—ENDOR spectroscopy was applied to get information on the localization of the spin. The electronic structure of Chl *a*⁺ is sensitive to environmental changes, for example, ligation, hydrogen bonding, and electrostatic interactions (46). Likewise, the spin density distribution in P700⁺ can be perturbed by environmental effects, conformational changes of the chlorine ring, or changes in the distance and relative orientation of the two Chls constituting P700. ENDOR spectroscopy applied to P700⁺ leads to an assignment of proton hfcs of the spin carrying Chl, P_B (12, 13). Unfortunately, an assignment of the hfcs of P_A has not been achieved so far. Compared with monomeric Chl *a*⁺ in organic solvents, the hfcs of the 12- and 2-methyl groups of P700⁺ are reduced, whereas the hfc of the 7-methyl group is increased (13). It has been argued that the all over decrease of spin density on P_B as compared with monomeric Chl *a*⁺ in organic solvents reflects a delocalization of spin density between the two halves of P700, and it has been estimated that at least 85% of the spin density is localized on P_B (13). Comparison of the hfcs of the methyl groups shows essentially no difference among the different species giving evidence that the electronic structure of P700⁺ is the same for all organisms. The same observation holds for different preparations from different *C. reinhardtii* strains (47) showing that the electronic structure of the P700⁺ is not susceptible to different preparation methods. However, studies on mutant reaction centers have shown that the spin density distribution can be specifically influenced by mutations that have a direct influence on the primary donor in bacterial reaction centers (48) or PS I (12, 17). ENDOR studies have been performed with mutants in which the axial His ligands to P_A and P_B were substituted by

several other amino acid residues. They revealed that only mutations to P_B lead to changes in the spectra, whereby only changes of the hfc of the 12-methyl group were resolved. This increase of only one hfc has been interpreted as a modification of the local environment of this methyl group (12). In contrast, mutations where the hydrogen bond to the 13¹ keto group of P_A was removed led to changes of the hfc's of the other half of the dimer P_B which was explained by a spin density shift from P_B toward P_A. The observed redistribution could therefore be taken as evidence for an electronic coupling between the two halves of the dimer as this was the first time that a mutation specifically affecting P_A showed an influence on the hfc's attributed to P_B. This could be rationalized within a dimer model that was originally proposed for the primary donor of the bacterial reaction center (17). The ENDOR results for the different mutants are also summarized in Table I. The changes in the hfc's of the different methyl groups of the mutants WA, WY, and WH A679 are very close to the error limit. It seems that the substitutions of Trp-A679 do not significantly affect the electron density distribution and that the slight changes might be the result of only minor perturbations in the surrounding of P700, because the distance between this Trp residue and the 7-methyl group is only about 4 Å. In contrast, mutations of Tyr-B659 display a larger effect on the hfc of the 12-methyl group comparable with the ones observed for the mutation of the axial His ligands. Conformational changes of the chlorine ring of the spin carrying Chl P_B have been proposed as an explanation for these results (12). Likewise, it can be speculated that substitution of Tyr-B659 by His or Ala induces a slight conformational change. On the other hand, the ZFS parameters for all the mutants under study calculated from the ADMR spectra (data not shown) are only slightly different (less than 1%) from the values previously obtained (17) for native PS I from *C. reinhardtii* ($|D| = 0.0280 \text{ cm}^{-1}$; $|E| = 0.0039 \text{ cm}^{-1}$). The small conformational distortions possibly caused by the mutations can probably not be revealed by changes of the ZFS parameters. The question of the triplet state location still remains to be clarified due to the lack of effects on these parameters induced by variations in the P700 protein environment either on the PsaA or PsaB subunit (12, 49).

If we assume that Tyr-B659 donates a hydrogen bond to the keto group of the phytol side chain of P_B, mutating this residue will lead to the removal of the hydrogen bond. As the phytol side chain does not belong to the conjugated π -orbital system, a specific effect of the hydrogen bond on this π -system can be excluded. However, the hydrogen bond might keep the phytol side chain in a certain conformation. Upon breakage of the hydrogen bond the phytol side chain might become more flexible leading to slight conformational changes of the chlorine ring and concomitantly to a redistribution of spin density within the macrocycle of P_B. Interestingly, the hfc's for the methyl groups of *C. reinhardtii* and *T. elongatus* are essentially the same, although it is exactly the residue at position B659 that is different for the two organisms. Although Trp is not a hydrogen bond donor, it might be able to keep the phytol side chain in a certain position due to its size. This is in contrast to the Ala or His mutations in *C. reinhardtii* where not only the hydrogen bond is broken but both residues are smaller. This is also in line with the fact that Ala is the smallest residue showing the largest effect.

The relatively small differences between the hfc's for the different species can be rationalized by the fact that the cation is mainly localized on one of the two Chls constituting P700. In contrast, the delocalization of the excited singlet states over the six Chls of the P700 reaction center may explain the suscepti-

bility of the optical properties to slight structural differences in the various species.

In summary, all the deviations observed in the optical spectra and in the reaction center properties clearly suggest the presence of significant differences in the properties and geometrical arrangement of the cofactors in PS I from different species despite the high degree of sequence homology. Furthermore, the results obtained with site-directed mutagenesis show that the deviations observed cannot be put down to single non-conserved amino acids in the vicinity of the cofactors. Such deviations could possibly be explained by long range effects due to variations of amino acids on PsaA and PsaB located further away which might slightly modify the protein-cofactor and cofactor-cofactor interactions. Therefore, it should be emphasized that the 2.5-Å structure of PS I from *T. elongatus* cannot be directly used for structurally based simulations of spectra and functional properties of PS I from other species.

Acknowledgments—We are grateful to Marianne Çetin, Heidi Pannier, and Claudia Schulz (Technische Universität Berlin) for excellent technical assistance. We thank Hanno Käss for the ENDOR measurements of different species and Ludwig Krabben and Uwe Fink for help in the initial stage of this work. We thank Margitta Dathe (Max-Delbrück-Center, Berlin-Buch, Germany) for the opportunity to use the CD spectrometer in her laboratory and for help with the CD measurements. We are also indebted to Matthias Rögner, University of Bochum, for providing PS I from *Synechocystis*.

REFERENCES

- Brettel, K. (1997) *Biochim. Biophys. Acta* **1318**, 322–373, and references therein
- Heathcote, P. (guest ed) (2001) *Biochim. Biophys. Acta* **1507**, and references therein
- Scheller, H. V., Jensen, P. E., Haldrup, A., Lunde, C., and Knoetzel, J. (2001) *Biochim. Biophys. Acta* **1507**, 41–60
- Manna, P., and Chitnis, P. R. (1999) in *Function and Molecular Genetics of Photosystem I in Concepts in Photobiology: Photosynthesis and Photomorphogenesis* (Singhal, G. S., Renger, G., Sopory, S. K., Irrgang, K. D., and Govindjee, eds) Narosa Publishing House, New Delhi, India
- Fromme, P., Schlodder, E., and Jansson, S. (2003) in *Light-harvesting Antennas in Photosynthesis* (Green, B., and Parson, W. W., eds) pp. 253–279, Kluwer Academic Publishers Group, Dordrecht, Netherlands
- Baymann, F., Brugna, M., Mühlenhoff, U., and Nitschke, W. (2001) *Biochim. Biophys. Acta* **1507**, 291–310
- Rochaix, J.-D. (2001) *Plant Physiol.* **127**, 1394–1398
- Jordan, P., Fromme, P., Witt, H. T., Klukas, O., Saenger, W., and Krauss, N. (2001) *Nature* **411**, 909–917
- Guergova-Kuras, M., Boudreaux, B., Joliot, A., Joliot, P., and Redding, K. (2001) *Proc. Natl. Acad. Sci. U. S. A.* **98**, 4437–4442
- Xu, W., Chitnis, P., Valieva, A., van der Est, A., Brettel, K., Guergova-Kuras, M., Pushkar, J., Zech, S. G., Stehlik, D., Shen, G., Zybaïlov, B., and Golbeck, J. H. (2003) *J. Biol. Chem.* **278**, 27876–27887
- Käss, H. (1995) *Die Struktur des primären Donators P700 in Photosystem I*, Ph.D. thesis, Technical University, Berlin
- Krabben, L., Schlodder, E., Jordan, R., Carbonera, D., Giacometti, G., Lee, L., Webber, A. N., and Lubitz, W. (2000) *Biochemistry* **39**, 13012–13025
- Käss, H., Fromme, P., Witt, H. T., and Lubitz, W. (2001) *J. Phys. Chem. B* **105**, 1225–1239, and references therein
- Webber, A. N., and Lubitz, W. (2001) *Biochim. Biophys. Acta* **1507**, 61–79
- Hiyama, T., and Ke, B. (1972) *Biochim. Biophys. Acta* **267**, 160–171
- Pålsson, L.-O., Flemming, C., Gobets, B., van Grondelle, R., Dekker, J. P., and Schlodder, E. (1998) *Biophys. J.* **74**, 2611–2622
- Witt, H., Schlodder, E., Teutloff, C., Niklas, J., Bordignon, E., Carbonera, D., Kohler, S., Labahn, A., and Lubitz, W. (2002) *Biochemistry* **41**, 8557–8569
- Redding, K., MacMillan, F., Leibl, W., Brettel, K., Hanley, J., Rutherford, A. W., Breton, J., and Rochaix, J.-D. (1998) *EMBO J.* **17**, 50–60
- Hippler, M., Redding, K., and Rochaix, J.-D. (1998) *Biochim. Biophys. Acta* **1367**, 1–62
- Harris, E. (1989) *Chlamydomonas Sourcebook*, pp. 25–64, Academic Press, San Diego
- Leibl, W., Brettel, K., Nabedryk, E., Breton, J., Rochaix, J.-D., and Redding, K. (1998) in *Photosynthesis: Mechanisms and Effects* (Garab, G., ed) Vol. 1, pp. 595–598, Kluwer Academic Publishers Group, Dordrecht, Netherlands
- Cui, L., Bingham, S. E., Kuhn, M., Käss, H., Lubitz, W., and Webber, A. N. (1995) *Biochemistry* **34**, 1549–1558
- van der Lee, J., Bald, D., Kwa, S. L. S., van Grondelle, R., Roegmer, M., and Dekker, J. P. (1993) *Photosynth. Res.* **35**, 311–321
- Kruip, J., Karapetyan, N. V., Terekhova, I. V., and Roegner, M. (1999) *J. Biol. Chem.* **274**, 18181–18188
- Fromme, P., and Witt, H. T. (1998) *Biochim. Biophys. Acta* **1365**, 175–184
- Kruip, J., Boekema, E. J., Bald, D., Boonstra, A. F., and Roegner, M. (1993) *J. Biol. Chem.* **268**, 23353–23360
- Porra, R. J., Thompson, W. A., and Kriedemann, P. E. (1989) *Biochim. Biophys. Acta* **975**, 384–394
- Schlodder, E., Paul, A., and Cetin, M. (2001) in *PS2001 Proceedings of the 12th*

- International Congress on Photosynthesis, Brisbane, Australia, August 18–23, 2001*, CSIRO Publishing, Melbourne, Australia
29. Rautter, J., Lenzian, F., Lubitz, W., Wang, S., and Allen, J. P. (1994) *Biochemistry* **33**, 12077–12084
 30. Carbonera, D., Collareta, P., and Giacometti, G. (1997) *Biochim. Biophys. Acta* **1322**, 115–128
 31. Kwa, S. L. S., Völker, S., Tilly, N. T., van Grondelle, R., and Dekker, J. P. (1994) *Photochem. Photobiol.* **59**, 219–228
 32. Gillie, J. K., Lyle, P. A., Small, G. J., and Golbeck, J. H. (1989) *Photosynth. Res.* **22**, 233–246
 33. Rutherford, A. W., and Mullet, J. E. (1981) *Biochim. Biophys. Acta* **13**, 225–235
 34. Angerhofer, A. (1991) in *Chlorophylls* (Scheer, H., ed) pp. 945–991, CRC Press, Inc., Boca Raton, FL
 35. Philipson, K. D., Sato, V. L., and Sauer, K. (1972) *Biochemistry* **11**, 4591–4595
 36. Cometta, A., Zucchelli, G., Karapetyan, N. V., Engelmann, E., Garlaschi, F. M., and Jennings, R. C. (2000) *Biophys. J.* **79**, 3235–3243
 37. Byrdin, M., Jordan, P., Krauss, N., Fromme, P., Stehlik, D., and Schlodder, E. (2002) *Biophys. J.* **83**, 433–457
 38. Setif, P., Mathis, P., and Vänngard, T. (1984) *Biochim. Biophys. Acta* **767**, 404–414
 39. Schlodder, E., Falkenberg, K., Gergeleit, M., and Brettel, K. (1998) *Biochemistry* **37**, 9466–9476
 40. Sonoike, K., and Katoh, S. (1989) *Biochim. Biophys. Acta* **976**, 210–213
 41. Flemming, C. (1995) *Charakterisierung der Antennensysteme von monomeren und trimeren Photosystem I Komplexen*, Thesis, Technical University, Berlin
 42. Gobets, B., van Stokkum, I. H. M., Rögner, M., Kruij, J., Schlodder, E., Karapetyan, N. V., Dekker, J. P., and van Grondelle, R. (2001) *Biophys. J.* **81**, 407–424
 43. Shubin, V. V., Karapetyan, N. V., and Krasnovsky, A. A. (1986) *Photosynth. Res.* **9**, 3–12
 44. Schwabe, T. M. E., and Kruij, J. (2000) *Indian J. Biochem. Biophys.* **37**, 351–359
 45. Williams, J. C., Alden, R. G., Murchison, H. A., Peloquin, J. M., Woodbury, N. W., and Allen, J. P. (1992) *Biochemistry* **31**, 11029–11037
 46. Lubitz, W. (1991) in *Chlorophylls* (Scheer, H., ed) pp. 903–944, CRC Press, Inc., Boca Raton, FL
 47. Krabben, L. (1999) *Die Protein-Umgebung des primären Donators P700 im Photosystem I: Biochemische und biophysikalische Charakterisierung von Mutanten der Grünalge Chlamydomonas reinhardtii*, Ph.D. thesis, Technical University, Berlin
 48. Rautter, J., Lenzian, F., Schulz, C., Fetsch, A., Kuhn, M., Lin, X., Williams, J. C., Allen, J. P., and Lubitz, W. (1995) *Biochemistry* **34**, 8130–8143
 49. Breton, J. (2001) *Biochim. Biophys. Acta* **1507**, 180–193
 50. Huber, M., Lenzian, F., Lubitz, W., Tränkle, E., Möbius, K., and Wasielewski, M. R. (1986) *Chem. Phys. Lett.* **132**, 467–473